

# Fracture Processes Observed with A Cryogenic Detector

J. Åström<sup>6</sup>, P.C.F. Di Stefano<sup>1,8</sup>, F. Pröbst<sup>1</sup>, L. Stodolsky<sup>1\*</sup>, J. Timonen<sup>7</sup>, C. Bucci<sup>4</sup>,  
S. Cooper<sup>3</sup>, C. Cozzini<sup>1</sup>, F. v. Feilitzsch<sup>2</sup>, H. Kraus<sup>3</sup>, J. Marchese<sup>3</sup>, O. Meier<sup>1</sup>,  
U. Nagel<sup>2,9</sup>, Y. Ramachers<sup>10</sup>, W. Seidel<sup>1</sup>, M. Sisti<sup>1</sup>, S. Uchaikin<sup>1,5</sup>, L. Zerle<sup>1</sup>  
<sup>1</sup> *Max-Planck-Institut für Physik, Föhringer Ring 6, D-80805 Munich, Germany;* <sup>2</sup> *Technische Universität München, Physik Department, D-85747 Munich, Germany;* <sup>3</sup> *University of Oxford, Physics Department, Oxford OX1 3RH, UK;* <sup>4</sup> *Laboratori Nazionali del Gran Sasso, I-67010 Assergi, Italy;* <sup>5</sup> *Joint Institute for Nuclear Research, Dubna, 141980, Russia;* <sup>6</sup> *CSC - IT Center for Science, P.O.Box 405, FIN-02101 Esbo, Finland;* <sup>7</sup> *Department of Physics, P.O. Box 35 (YFL), FIN-40014 University of Jyväskylä, Finland;* <sup>8</sup> *Institut de Physique Nucléaire de Lyon, Université Claude Bernard Lyon I, 4 rue Enrico Fermi, 69622 Villeurbanne Cedex, France;* <sup>9</sup> *Institute of Chemical Physics and Biophysics, EE-0026 Tallinn, Estonia;* <sup>10</sup> *University of Warwick, Dept. of Physics, Coventry CV4 7AL, UK, \* Corresponding author, email address: les@mppmu.mpg.de.*

In the early stages of running of the CRESST dark matter search using sapphire detectors at very low temperature, an unexpectedly high rate of signal pulses appeared. Their origin was finally traced to fracture events in the sapphire due to the very tight clamping of the detectors. During extensive runs the energy and time of each event was recorded, providing large data sets for such phenomena. We believe this is the first time the energy release in fracture has been directly and accurately measured on a microscopic event-by-event basis. The energy threshold corresponds to the breaking of only a few hundred covalent bonds, a sensitivity some orders of magnitude greater than that of previous technique.

We report some features of the data, including energy distributions, waiting time distributions, autocorrelations and the Hurst exponent. The energy distribution appear to follow a power law,  $dN/dE \propto E^{-\beta}$ , similar to the power law for earthquake magnitudes, and after appropriate translation, with a similar exponent. In the time domain, the waiting time  $w$  or gap distribution between events has a power law behavior at small  $w$  and an exponential fall-off at large  $w$ , and can be fit  $\propto w^{-\alpha} e^{-w/w_0}$ . The autocorrelation function shows time correlations lasting for substantial parts of an hour. An asymmetry is found around large events, with higher count rates after, as opposed to before, the large event .

## INTRODUCTION

In the Spring of 1999 preliminary runs of the CRESST dark matter search [1] were carried out at the Gran Sasso Laboratory (LNGS), a deep underground laboratory for low background physics located in the Apennines. In these first runs of CRESST a phenomenon was observed which we believe may be of interest for the study of crack and fracture formation in brittle materials. CRESST is a cryogenic detector, working in the vicinity of 10 milli-Kelvin [2]. In addition to being deep underground for shielding against cosmic rays, it is carefully designed to minimize effects of radioactive background. The detector elements were large (262 gram) high quality single crystals of sapphire, with a strip of superconductor (W) evaporated on one surface to serve as a sensitive thermometer. This system, as shown by tests with gamma ray sources, detects single events in the sapphire with energies in the range from about 1 keV to several hundred keV with good energy resolution ( 0.5 keV) and good time resolution (40 or 100  $\mu$ s for the onset of a pulse).

In order to reach these low temperatures it is important to eliminate the effects of any vibrations (“micro-

phonics”) that might deliver energy to the crystal. Thus in addition to special suspensions to isolate the apparatus, the crystals are held very tightly in their holders to prevent any even microscopic frictional effects. In the data to be discussed here this was effected by small sapphire balls held against the sapphire crystal by a plastic clamp. The plastic of the clamp, delrin, is known to contract substantially at low temperature, thus providing additional “tight holding”. An unanticipated result of the small contact area of the hard sapphire balls and the great force of the clamp turned out to be a cracking or fracturing of the sapphire. This was observed as follows.

When the system was first brought into operation, an unexpectedly high rate of signal pulses was observed. Initial fears that this might be due to an unexpected radioactive contamination were relieved by the observation that even an unknown radioactive contamination must be Poisson distributed in time, while the unexpected pulses appeared rather to come in “bursts” or “avalanches”. Examination of the time distributions showed that they were indeed non-Poissonian.

*Pulse formation and fractures:* The pulses themselves resembled those seen from good particle events. However,

this is a rather unspecific criterion, due to the operating characteristics of the detector. There are essentially three steps in the production of a signal pulse 1) A relatively localized energy release within a short time, 2) A rapid degradation of this energy into a uniform “hot” ( $\sim 10^{\circ}K$ ) gas of phonons produced through phonon-phonon interaction and decay, as well as interaction with the crystal surface, 3) Absorption of the phonons in the thermometer strip. This leads to a heating with an increase of electrical resistance for the superconductor, which is finally read out by SQUID electronics. The resulting pulse shape is well described by a model employing the various thermal and electrical parameters of the system [3]. As may be seen from this brief description, the pulse shape is essentially determined by the thermal responses of the system and not by the initiating event, as long as it is “fast”. Hence any release of a given energy in the crystal in a short time ( $\mu$  seconds) leads to the same pulse shape and so examination of the pulses does not lead to an identification of their origin. An extensive search for the origin of the pulses was finally successful when it was noticed that there appeared to be markings or scratches on the crystal at the contact points with the sapphire balls. When the sapphire balls were replaced by plastic stubs, which are evidently much softer, the event rate immediately dropped from some thousands per hour to the expected few per hour.

These observations strongly suggest that the pulses were due to some kind of cracking or micro-fracturing phenomena in the sapphire crystal and/or its support balls. Indeed, examination under a microscope revealed a small crater with radiating irregular fissures extending sideways and down into the crystal. Damage to the sapphire balls was also observed. Since the reduction in rate after the exchange of the sapphire balls was so large, we believe the data taken with the sapphire balls are essentially all fracture events. If we accept this crack or fracture hypothesis, our data then represent a large sample of well measured fracture events, under low background conditions, and with good time and energy determination.

*Calibration runs:* In order to calibrate the energy scale regular calibration runs were carried out. In these runs the system is left undisturbed and a radioactive source supplying 120 keV photons (which can penetrate to the detectors) is inserted in an external plug in the shielding. These photon-induced events can be selected by using the resulting 120 keV peak in the data. Since a radioactive source produces statistically independent events, that is Poisson statistics, these events provide a useful comparison when studying statistical properties of the data.

## ENERGY DISTRIBUTIONS

We believe this is the first time that the energy release in microfracture has been accurately measured on a microscopic event-by-event basis.

It is to be emphasized that the cryogenic method provides an *absolute* measurement of the *total* energy release in the fracture. This is to be contrasted with the study of acoustic emission in materials or seismic measurements of earthquakes. There the energy determination is necessarily indirect since there are various assumptions and uncertainties concerning production, propagation, and detection involved in translating the observed signals into the true energy of the event. On the other hand the cryogenic method, essentially calorimetric in character, is a direct measurement of the full energy. The energy scale is fixed by the calibration with known sources and the resulting accuracy of the CRESST energy determination is on the order of a few percent [1].

In addition to the directness of the energy measurement an important feature of the cryogenic method is its great sensitivity. The closest previous technique appears to be the study of acoustic emission in materials [4],[5]. There the smallest emitting region considered is on the order of a square micron [6]. This will correspond to the breaking of  $\sim 10^7$  bonds in the crystal. On the other hand, our energy threshold is typically some keV (Fig. 1). This corresponds to the breaking of only a few hundred or thousand bonds. Thus the cryogenic method appears to be many orders of magnitude more sensitive than previous technique. Small cryogenic devices can even be sensitive to energies in the eV range [2] and it is possible that studies of this type involving stress release of only a few atoms are feasible [7].

In Fig. 1 we show the differential distribution  $dN/dE$  for the number of events  $N$  per unit energy, for four data sets with two detectors from Run9. The straight line is the result of a power law fit

$$dN/dE \propto E^{-\beta} \quad (1)$$

to the lowest curve, which yields  $\beta \approx 1.9$ . Similar results are found from fits to other data sets. From a total of seven sets examined (from Runs 9, 10 and 11)  $\beta$  ranged between 1.7 and 2.0. An interesting point is that the rates do not appear to differ greatly from one data set to another, despite the fact that different crystals and mountings are often involved. At 21 keV for example, the rates over the various data sets vary between 4 and 11 pulses/keV-hr.

A power law of this type, called the Gutenberg-Richter law [8], is well known for the “magnitudes” of earthquakes. Unfortunately the “magnitude” is a seismic amplitude and not a direct measurement of the energy of an earthquake. Thus a simple comparison is not possible. However if one takes the prescription that the seismic

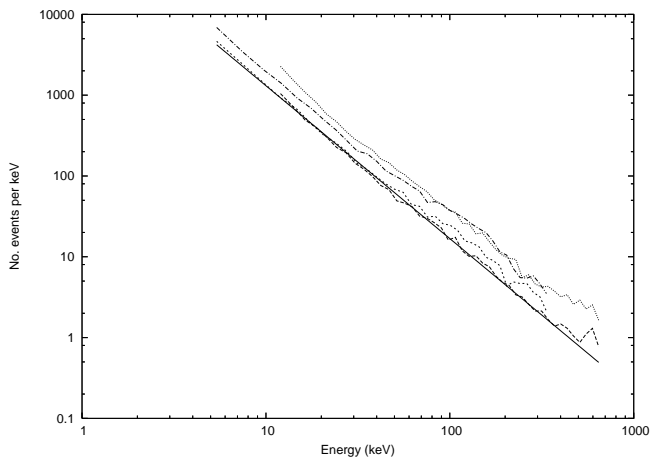


FIG. 1: Energy spectra from four data sets of Run9, with 53 hr for the upper pair of curves and 28hr for the lower. The straight line shows a fit to the lowest curve  $\propto E^{-\beta}$ , yielding  $\beta \approx 1.9$ .

amplitude to approximately the 3/2 power [8],[9] represents the energy, and uses the power  $\approx 1.0$  found for the *integral* distribution of earthquake magnitudes [9], it corresponds to  $\beta \approx 1 + \frac{2}{3} \approx 1.7$ , not far from our  $\beta \approx 1.7 - 2.0$ . Of course, the six orders of magnitude range available for seismic data is much greater than the one or two orders of magnitude available here.

It should also be noted that such power law, that is scale free, distributions appear in many phenomena, often related to an underlying fractal process [10]. In the acoustic emission recordings of microfracture events in brittle materials for example, such a distribution typically appears, with a somewhat lower exponent,  $\beta \approx 1.5$  [4].

## TIME SERIES

*Waiting Time Distributions:* A useful quantity in the study of intermittent data such as the present is the “waiting time”  $w$ . To each event  $i$  we assign  $w_i$ , the time interval till the next event, and study the distribution of these intervals. Fig. 2 shows the waiting time distribution for detector 2 in a 28 hr data set of Run 9. The distribution has power law behavior at small  $w$  and an exponential fall off at large  $w$ , and an accurate fit is obtained with  $dN/dw \propto w^{-\alpha} e^{-w/w_0}$ , with  $\alpha = 0.33$ . Similar results are found for other data sets with  $\alpha$  in the range 0.25-0.5. The parameter  $w_0$  determines the location of the crossover from power law to exponential and is essentially the inverse rate or average waiting time, with  $\bar{w} = (1 - \alpha)w_0$ . Qualitatively similar results, with  $\alpha$  near to or somewhat less than one, have been reported for earthquakes in California [11].

For the simple case of Poisson statistics, one expects

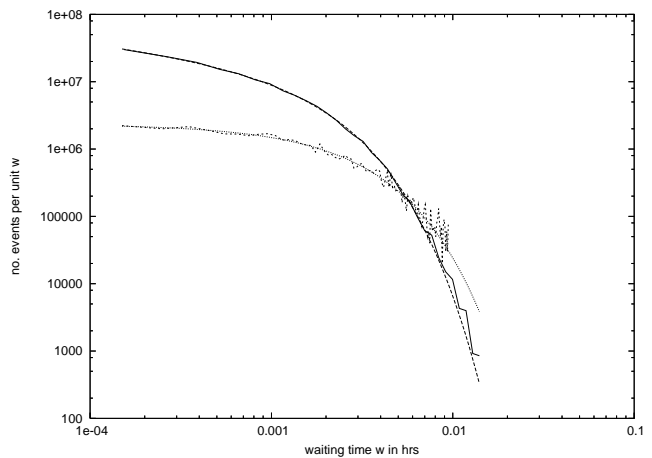


FIG. 2: Waiting time distributions. Upper curve: fractures, fit to  $\propto w^{-\alpha} e^{-w/w_0}$ . Lower curve: photon-induced events from a calibration run, fit to  $\propto e^{-w/w_0}$ .

a waiting time distribution  $\propto e^{-w/w_0}$ , where  $1/w_0$  is the average count rate. The lower curve of Fig. 2 shows the waiting time distribution for the photon-induced events of a calibration run, with a fit to  $\propto e^{-w/w_0}$ . As expected there is a good fit, and with  $1/w_0$  in agreement with the event rate.

An interesting point concerns the behavior of  $w_0$  for fracture events as the the energy threshold for the sample is raised. It appears that the form  $w^{-\alpha} e^{-w/w_0}$  is preserved, with  $\alpha$  varying little. Since the count rate is reduced however, the value of  $w_0$  increases and so the crossover between power law and exponential behavior moves to larger  $w$ . Indeed, taking a given data set (Run9-d2,100 $\mu$ s), repeatedly raising the energy threshold and fitting for  $w_0$ , we find a linear relation between the inverse count rate, that is  $\bar{w}$ , and the fitted  $w_0$ . The slope and the relation  $\bar{w} = (1 - \alpha)w_0$  then gives a global determination  $\alpha \approx 0.26$ .

The power law behavior for the waiting times at small  $w$ , as well as the power law for the energy distribution in the previous section, is suggestive of an underlying scale-free processes without any intrinsic dimensional parameter, as is common in fractal processes [10]. However this cannot be entirely true here since  $w_0$  is a time and has dimensions. Since  $e^{-w/w_0}$  corresponds in fact to a Poisson distribution, this may suggest an interpretation in terms of some basic scale free processes where several such processes are occurring independently and simultaneously and so are overlapping in the data. This arises trivially if the signals originate from more than one of the support points of the crystal, of which there were several; but one can also imagine independent crack systems beneath one support point.

The increase of  $w_0$  as the count rate goes down suggests that the limit of zero count rate is a kind of critical point: the waiting time becomes infinite as the distribu-

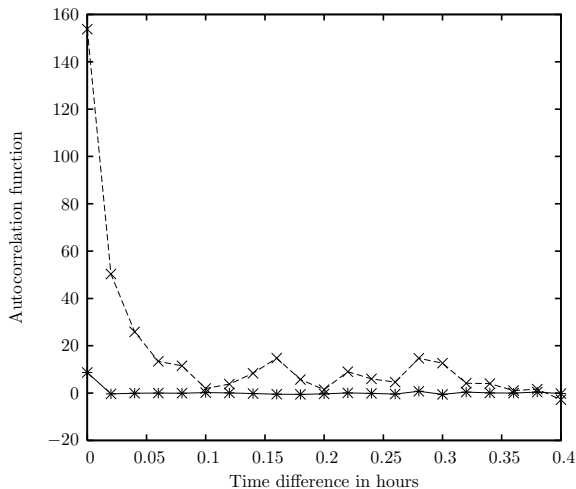


FIG. 3: Autocorrelation function  $C$  for the event rate from calibration data of Run10. The lower curve is for photon-induced events (events in the 120 keV peak), and the upper curve is for fractures plus some admixture of compton scatters (events below the peak). For the photons the data is consistent with  $C = 0$  for  $(t - t') \neq 0$  as expected for Poisson statistics, with  $C(0) = \text{Variance} = \bar{R}$ .

tion becomes non-integrable and completely scale free, while  $1/w_0$  appears as a diverging correlation length. Understanding  $w_0$  is an interesting point for further study.

*Correlations in Time:* We expect the existence of correlations in time, corresponding to the “bursts” or “avalanches”. We use the event rate  $R_t$  of a calibration run to construct the autocorrelation function

$$C(t - t') = \overline{(R_t - \bar{R})(R_{t'} - \bar{R})} \quad (2)$$

and compare  $C$  for photon-induced events and fractures in Fig. 3. While for photons we have  $C = 0$  as expected, for the microfractures there are correlations lasting for substantial fractions of an hour. These long-term correlations are found for the fracture events of all data sets. The physical origin of the correlations may be in stress relaxation phenomena where a slow “diffusion” of strain [12] can trigger new microfractures when meeting other weak spots in the crystal.

*Hurst exponent:* The autocorrelations as in Fig. 3 can be approximately fit to power laws  $\propto (t - t')^{-p}$ . As noted above, this is suggestive of the scale free, self-similar behavior associated with fractal statistics. A way of characterizing such behavior is in terms of what is called the Hurst exponent  $H$ ; and we can check the plausibility of such a description by comparing the consistency of  $H$  found in different ways. Table I shows  $H$  found in three ways for various data sets. First the autocorrelation exponent  $p$  is fitted to find  $H = 1 - p/2$ . The next column shows  $H$  determined by the “growth of the standard deviation”, a characterization of the fluctuations in the event rate  $\sim t^H$ , where  $t^{0.5}$  would be the classical gaussian or

TABLE I: Exponent  $H$  found by different methods. d1 and d2 refer to the two detectors in operation, and 40, 100  $\mu\text{s}$  to different digitization windows used in data taking in Run9.

| Data Set                  | Autocorr. | Std. Dvtn. | Sh. Entropy |
|---------------------------|-----------|------------|-------------|
| Run9 d1 100 $\mu\text{s}$ | 0.77      | 0.70       | 0.69        |
| Run9 d2 100 $\mu\text{s}$ | 0.80      | 0.80       | 0.80        |
| Run9 d1 40 $\mu\text{s}$  | 0.73      | 0.70       | 0.67        |
| Run9 d2 40 $\mu\text{s}$  | 0.69      | 0.70       | 0.65        |
| Run10 d2                  | 0.59      | 0.63       | 0.59        |
| Run11 d1                  | 0.60      | 0.64       | 0.53        |
| Run11 d2                  | 0.69      | 0.66       | 0.62        |

random walk behavior with finite range correlations. Finally, the last column gives  $H$  found from the “Shannon Entropy”, related to the probability of the number of events over a time interval  $t$  [13]. Although the fits were not all excellent and there is considerable fluctuation in the results, the overall rough consistency of the three determinations supports the picture of a scale free, self-similar process. We do not necessarily expect the same  $H$  for different data sets since these involve different energy thresholds and sensitivities.

## CLUSTERS

A frequently used concept in the earthquake literature is the “Omori Cluster”: a “big shock” followed by “aftershocks”. As Fig. 1 shows, and as is also the case for earthquakes, there is no separate class of high energy events—no distinctive “big shocks”. Naturally, as should be expected from the “avalanches” or correlations, given any event, there is a general increase in rate at nearby times. Although this increase is quite substantial, (a factor four with one second bins, see Fig. 4) this simply reflects the “bursts” or “avalanches” and is not specific to “big events”.

More specific to “big events”, however, we find a time asymmetry with respect to “before” and “after”. That is, there is on average more activity after, as opposed to before, “big events”. Fig. 4 shows the count rate from a data set of Run9, for times close to “big events”, with “after” (upper histogram) and “before” (lower histogram) plotted separately. “Big” was defined as a pulse with  $E > 300\text{keV}$ . The bin size is  $2.0 \times 10^{-4}\text{hr} = 0.72\text{s}$ . One notes a significantly higher rate in the first bin “after” relative to that in the first bin “before”. There is a reasonable fit to a power law for the decline in the rate toward the average value, and a significantly steeper power “after” relative to that “before” is found. Similar results are obtained for other data sets.

An asymmetry of this type appears to exist in seismic data and certain models [14] and seems to indicate that the “big events” tend to occur early in the “bursts”.

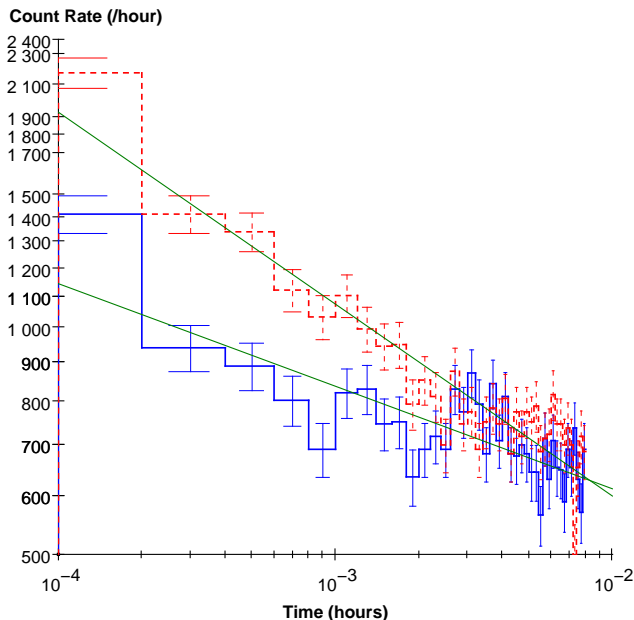


FIG. 4: Count rates in the vicinity of “big events”, showing a time asymmetry “before” and “after” the “big events”. From a 53 hr data set of Run9, plotted in 0.72 s bins. The upper (dotted,red) histogram is for times following the “big event” and the lower (solid,blue) histogram for times preceding the “big event”. The straight lines are power law fits, yielding a power  $0.13 \pm 0.01$  “before” and a power  $0.25 \pm 0.01$  “after”. There were 1082 “big events”, defined as a single pulse with  $E > 300\text{keV}$ . The average rate in the run was 526/hr.

### CRACK PROPAGATION AND MATERIAL PROPERTIES

Our material is a single crystal of high purity[15]. In crack propagation models the growing stress enhancement at the crack tip implies that a “hard spot” is necessary to limit the propagation of a crack; thus when a homogeneous stress is applied to a defect-free material there is nothing to stop a propagating crack. Presumably the microfractures here were limited by the random, non-homogeneous stress and defect field which quickly arises as fractures form in the pure material. This may have been assisted by the damage to the small sapphire balls, leading to an irregular application of the stress. Although we speak of “cracks”, it should be kept in mind that from our simple observation of pulses we cannot infer the exact nature of the microfracture. Finally, with respect to materials it should be noted that our system is of course quite opposite to those in the geological context, where one has highly heterogeneous systems, while here we have a very pure material.

### DEVELOPMENT OF THE TECHNOLOGY

It is interesting to contemplate the extension of this method in the study of fracture phenomena. The superconducting thermometer, and perhaps other cryosensors [2], can be applied to many materials. The very low temperature and large crystals of the dark matter search would not always be needed, and indeed it might be possible to follow the crack development in time with a smaller and thus faster system. However, low background conditions may still be necessary to avoid contamination of the data by non-fracture events. In the present data the crystal was contacted by several of the small sapphire balls, and we are unable to determine where an event originates. Such effects lead to a dilution of correlations, which thus may be intrinsically much stronger than appear here. In an apparatus especially designed for such studies one could arrange to have only one “hard” contact and with a known force. Finally, since the energy range available is relatively small compared to that for earthquakes it would be useful to consider techniques for increasing the dynamic range.

- 
- [1] For recent CRESST results on dark matter see G. Angloher *et al.*, astro-ph/0408006, *Astroparticle Phys.* **23**, 325 (2005). For the apparatus as it was in operation here, see M. Sisti *et al.*, *NIM* **A466** 499 (2001).
  - [2] For a general introduction to cryogenic detectors see L. Stodolsky, *Physics Today*, August, 1991 or N. Booth, B. Cabrera and E. Fiorini, *Ann. Rev. Nuclear and Particle Science* **46**, Dec 1996.
  - [3] F. Pröbst *et al.*, *Jnl. Low Temp. Physics* **100** 69 (1995).
  - [4] P. Diodati, F. Marchesoni, and S. Piazza, *Phys. Rev. Lett.* **67**, 2239 (1991); G. Caldarelli, F. D. Di Tolla, and A. Petri, *Phys. Rev. Lett.* **77**, 2503 (1996); A. Garcimartín, A. Guarino, L. Bellon, and S. Ciliberto, *Phys. Rev. Lett.* **79**, 3202 (1997); C. Maes, A. Van Moffaert, H. Frederix, and H. Strauven, *Phys. Rev. B* **57**, 4987 (1998).
  - [5] A useful overview of acoustic emission is given by L. M. Rogers in *Structural and Engineering Monitoring by Acoustic Emission Methods—Fundamentals and Applications*, Lloyd’s Register (2001).
  - [6] Rogers, ref [5] defines magnitude zero—the smallest event—as a microfracture of size  $1\mu\text{m}^2$ . The use of the square dimension stems from the slip-plane picture of the fracture.
  - [7] It is conceivable that such events have been detected as “excess noise” in certain cryodetectors. See the remarks by L. Stodolsky in *Proceedings LTD-11*, Tokyo 2005, to be published in *NIM*.
  - [8] *Seismicity of the Earth*, B. Gutenberg and C. F. Richter, Hafner Publishing Company, (1965).
  - [9] K. Christenson, L. Danon, T. Scalon, and P. Bak, *Proceedings National Academy of Sciences* **99** suppl.1, 2509, 2002.
  - [10] A general review of such concepts may be found in B. J. West, M. Bologna, and P. Grigolini *Physics of Fractal*

*Operators*, Springer-Verlag (2003).

- [11] N. Scafetta and B. J. West, Phys. Rev. Lett. 92, 138501 (2004)
- [12] M. S. Mega et al, Phys. Rev. Lett. 90, 188501 (2003).
- [13] N. Scafetta and P. Grigolini Phys. Rev. **E 66**, 036130 (2002). For these issues in the geological context see *Fractals and Dynamic Systems in Geoscience* J. Kruhl, Ed. Springer-Verlag (1994).
- [14] A. Helmstetter, S. Hergarten , and D. Sornette Phys. Rev **E70** 046120 (2004).
- [15] The crystals were high quality single crystals, optically defect free. One was supplied by the Hemex company, the other by BEC Breznikar.